RESEARCH ARTICLE

# Cortical and Corticomuscular Beta-Gamma Phase-Amplitude Coupling During Different Locomotion States and the Effects of Levodopa in Parkinson's Disease

Haifeng Zhao, PhD,[1,2,3,4] Shenglin Hao, BS,[1] Peiran Zhang, BS,[1] Shenghong He, PhD,[5] Laura Wehmeyer, PhD,[5] Ziyi Feng, MS,[1] Lu Xu, BS,[1] Shikun Zhan, MD,[1] Wei Liu, MD,[1] Xiaoxiao Zhang, MD,[1] Marie-Laure Welter, PhD,[6,7] Dianyou Li, MD,[1] Bomin Sun, MD,[1] Yong Lu, MD,[2,3,4*] Huiling Tan, PhD,[5*] and Chunyan Cao, PhD[1*]

**ABSTRACT: Background:** Phase-amplitude coupling (PAC) in the beta-gamma range has emerged as a promising electrophysiological biomarker of Parkinson's disease (PD).
**Objective:** This study aims to investigate how levodopa and locomotion modulate cortical (central electroencephalogram [cEEG]) and corticomuscular (cEEG-gEMG [gastrocnemius electromyography]) beta-gamma PAC in patients with PD.
**Methods:** Thirty patients with PD underwent simultaneous cEEG and gEMG recordings during sitting, standing, and free walking in both *off* and *on* dopaminergic states. Spectral features and PAC analyses were conducted to assess the effects of levodopa, locomotion, and their associations with motor symptoms.
**Results:** In the *off* levodopa state, patients showed prolonged gait cycle intervals and shorter step lengths, correlating with higher Movement Disorder Society–revised Unified Parkinson's Disease Rating Scale Part III (UPDRS-III) scores. The cEEG beta-gamma PAC during sitting and standing, and cEEG-gEMG beta-gamma PAC during walking, positively correlated with UPDRS-III in the *off* levodopa state. The cEEG alpha/low beta-gamma and cEEG-gEMG low beta-gamma PAC increased from *on* to *off* levodopa while walking, with the latter correlating with reduced step length. Step event–related PAC analysis unveiled a dynamic enhancement of alpha/beta cEEG-gamma gEMG PAC around heel strikes in *on* levodopa compared with *off*.
**Conclusions:** Both cortical and corticomuscular beta-gamma PACs are modulated by levodopa and locomotion, with low beta-gamma corticomuscular PAC specifically linked to gait dysfunction. Moreover, the levodopa-related enhancement of alpha/beta–gamma PAC during heel strikes highlights the functional relevance of dopaminergic modulation during gait. These findings highlight the potential of PAC as a biomarker for PD, particularly in the development of gait phase-locked adaptive deep brain stimulation strategies for patients with PD guided by noninvasive PAC monitoring. © 2025 The Author(s). *Movement Disorders* published by Wiley Periodicals LLC on behalf of International Parkinson and Movement Disorder Society.

**Key Words:** Parkinson's disease; phase-amplitude coupling; gait dysfunction; motor cortex; corticomuscular connectivity

[1]Department of Functional Neurosurgery, Affiliated Ruijin Hospital, Shanghai Jiao Tong University School of Medicine, Shanghai, China; [2]Department of Radiology, Affiliated Ruijin Hospital, Shanghai Jiao Tong University School of Medicine, Shanghai, China; [3]Clinical Neuroscience Center, Affiliated Ruijin Hospital, Shanghai Jiao Tong University School of Medicine, Shanghai, China; [4]Clinical Neuroscience Center, Affiliated Ruijin Hospital Luwan Branch, Shanghai Jiao Tong University School of Medicine, Shanghai, China; [5]MRC Brain Network Dynamics Unit, Nuffield Department of Clinical Neurosciences, University of Oxford, Oxford, United Kingdom; [6]Paris Brain Institute, CNRS UMR 7225, INSERM 1127, Sorbonne University, Paris, France; [7]Neurophysiology Department, CHU Rouen, Rouen University, Rouen, France



*Correspondence to: Chunyan Cao and Yong Lu, Affiliated Ruijin Hospital, Shanghai Jiao Tong University School of Medicine, 197 Ruijin Second Road, Shanghai 20025, China. E-mails: E-mail: ccy40646@rjh.com.cn (C.C.) and E-mail: 18917762053@163.com (Y.L.)
Huiling Tan, MRC Brain Network Dynamics Unit, Nuffield Department of Clinical Neurosciences, University of Oxford, Oxford OX1 3TH, UK. E-mail: huiling.tan@ndcn.ox.ac.uk

Haifeng Zhao, Shenglin Hao, and Peiran Zhang contributed equally to this work.

Yong Lu, Huiling Tan, and Chunyan Cao contributed equally to this work.

**Relevant conflicts of interest/financial disclosures:** S.H., L.W., and H.T were supported by the Medical Research Council (MRC) (MC_UU_00003/2), the Medical and Life Sciences Translational Fund (MLSTF) from the University of Oxford, the National Institute for Health and Care Research (NIHR) Oxford Biomedical Research Centre, and the Rosetrees Trust, UK. S.H. was also supported by a Non-Clinical Postdoctoral Fellowship from the Guarantors of Brain and an International Exchanges Award (IES\R3 \213,123). No conflicts of interest to report.

**Funding agencies:** This work was supported by the Postdoctoral Fellowship Program of CPSF under Grant GZC20231665 (to H.Z.), Shanghai Municipal Science and Technology Commission (21Y11905300 to B.S.), and the National Science Foundation of China (82071547 to C.C.).

Full financial disclosures and author roles may be found in the online version of this article.

**Received:** 22 May 2025; **Revised:** 6 July 2025; **Accepted:** 18 August 2025

**Published online 6 September 2025 in Wiley Online Library (wileyonlinelibrary.com). DOI: 10.1002/mds.70031**

Parkinson's disease (PD) impairs motor function because of dopaminergic neuron loss in the substantia nigra, leading to symptoms such as tremor, bradykinesia, rigidity, and postural instability. Although clinical evaluation by medical doctors remains the gold standard for PD diagnosis and assessment,[1,2] it is highly dependent on clinician's experience and lacks continuous monitoring of symptom fluctuations throughout the day.[3] Electrophysiological biomarkers, such as beta and gamma oscillations in subcortical local field potentials, electroencephalographic (EEG) or magnetoencephalographic (MEG) measurements, and electromyography (EMG), offer objective insights into PD-related neural disruptions and hold promise for diagnosis and assessment.[4] Elevated beta power in basal ganglia, such as subthalamic nucleus (STN) and globus pallidus interna (GPi), has been well established as a hallmark for PD.[5,6] Abnormal beta bursts are associated with motor symptoms such as bradykinesia and rigidity,[7] reflecting pathological beta hypersynchronization that disrupts normal motor function.[5,8] Meanwhile, a finely tuned gamma activity becomes more prominent with dopamine therapy[9] and can be entrained by deep brain stimulation (DBS).[10] These insights have guided therapeutic strategies like DBS, which aim to reduce beta and enhance gamma activity in the basal ganglia.[5,11-13] However, beta-gamma power changes in the cortex, particularly when measured noninvasively using EEG or MEG, remain inconsistent.[14-18]

Meanwhile, phase-amplitude coupling (PAC), which describes the modulation of higher-frequency oscillations by the phase of lower-frequency rhythms, holds promise for understanding cross-frequency interactions in the brain. Previous studies have shown that PAC in the STN and GPi, involving motor-relevant frequencies, such as beta, coupled with high-frequency gamma (40–200 Hz) oscillations, reflects the pathological synchronization seen in PD.[19-23] In addition, enhanced beta-gamma PAC in the primary and sensorimotor cortex has been proposed as a biomarker for PD, because it correlates with motor symptoms[24-26] and reduces with dopamine medication[27] and DBS.[28] Notably, cortical PAC has also been linked to freezing of gait (FOG). One study using Electrocorticography (ECoG) reported increased beta-gamma PAC in the motor cortex during FOG,[29] whereas another study recording scalp EEG found gradually increased PAC in the sensorimotor area during gait preparation when FOG symptoms worsened.[30] These findings suggest that cortical PAC may serve as a biomarker for FOG, potentially informing new strategies to prevent falls in patients with PD. However, despite these insights, it remains unclear how cortical beta-gamma PAC is modulated by different locomotion states and dopaminergic medication.

Moreover, to better understand how these neural dynamics relate to actual motor function, it is essential to not only examine cortical activity but also its coupling with muscular output. The mechanisms by which cortical activity couples to muscle output remain insufficiently understood. Although limited studies[31-34] have investigated cross-region coherence between the cortex, basal ganglia, and muscles, cross-frequency coupling between cortex and muscle has been largely unexplored. For example, reductions in beta band corticomuscular coherence (CMC) in PD have been reported,[32,33] while increases in gamma band CMC have been observed during muscle contractions[35] and dynamic force controls.[36] However, the role of cross-frequency corticomuscular coupling across different locomotion contexts remains unstudied, yet this could offer valuable insights into how cortical activity influences muscle output.

Our study aims to address these knowledge gaps by employing simultaneous noninvasive EEG and EMG recordings across multiple locomotion states (sitting, standing, and free walking) in PD patients with medication both *on* and *off*. Footpad sensors track key events, such as heel-strike and toe-off, within each step cycle during free walking. This approach enables us to investigate the role of beta-gamma PAC in the central EEG (cEEG) and corticomuscular coupling across different motor states, as well as to explore step-related modulations. In addition, we aim to assess correlations between PAC and clinical measures of motor disability and gait instability, and to examine how levodopa (L-dopa) administration modulates both cortical PAC and corticomuscular coupling.

## Patients and Methods

### Participants and Ethical Approval

This study was approved by the Ethics Committee of Ruijin Hospital, Shanghai Jiao Tong University School of Medicine. Thirty participants with PD (18 males), aged 52 to 76 ($63.97 \pm 6.97$) years, took part in the study. The participants were assessed under both *off* and *on* dopaminergic treatments, as indicated in Table 1. The Movement Disorder Society–revised Unified Parkinson's Disease Rating Scale Part III (UPDRS-III) score varied across participants from 26 to 101 in the *off* state ($57.36 \pm 13.53$) and from 9 to 68 in the *on* state ($33.65 \pm 12.88$), with a mean improvement of 41.34% after dopaminergic treatment (Table 1). The UPDRS-III assessments were performed by professional clinicians before the study according to MDS-UPDRS guidelines set by the International Parkinson and Movement Disorder Society. The scale was organized into specific subsections for detailed analysis, such as rigidity (3.2–3.3), akinesia (3.4–3.14), tremor (3.15–3.18), and gait problems (3.10–3.14). The Hoehn and Yahr stage, patient age, and PD

**TABLE 1** *Participant demographics*

| Patient No./Gender | Age/Duration (y) | UPDRS-III score | | | HY stage | LED dose (mg/day) |
|---|---|---|---|---|---|---|
| | | Total (*off*/*on*) | Gait (*off*/*on*)[a] | FOG (*off*/*on*)[a] | | |
| 1/M | 65/3 | 52/32 | 2/1 | 0/0 | 2.5 | 400 |
| 2/M | 66/10 | 101/68 | 2/1 | 2/0 | 3 | 1200 |
| 3/F | 62/8 | 44/27 | 2/3 | 0/0 | 3 | 1147.5 |
| 4/M | 74/8 | 69/46 | 2/2 | 2/2 | 2.5 | 600 |
| 5/M | 76/3 | 64/44 | 2/1 | 1/0 | 2.5 | 150 |
| 6/M | 56/4 | 64/31 | 2/0 | 0/0 | 2.5 | 875 |
| 7/F | 54/8 | 50/32 | 1/0 | 0/0 | 2 | 225 |
| 8/F | 67/2 | 61/41 | 2/1 | 0/0 | 2.5 | 525 |
| 9/M | 56/2 | 41/25 | 2/1 | 0/0 | 2.5 | 375 |
| 10/M | 63/20 | 49/11 | 2/2 | 2/0 | 2.5 | 1800 |
| 11/M | 70/14 | 49/24 | 1/0 | 0/0 | 2.5 | 1200 |
| 12/F | 74/5 | 78/47 | 3/2 | 4/1 | 3 | 200 |
| 13/F | 71/7 | 54/33 | 3/3 | 2/1 | 3 | 1800 |
| 14/M | 70/8 | 76/37 | 2/0 | 2/0 | 3 | 848.25 |
| 15/M | 68/3 | 65/42 | 2/1 | 2/0 | 2.5 | 350 |
| 16/M | 57/6 | 61/33 | 2/1 | 2/0 | 2.5 | 873.25 |
| 17/M | 58/4 | 48/24 | 2/0 | 0/0 | 2.5 | 575 |
| 18/M | 67/20 | 81/60 | 3/2 | 2/2 | 4 | 600 |
| 19/F | 61/12 | 72/32 | 3/1 | 2/2 | 3 | 650 |
| 20/F | 54/6 | 54/26 | 2/1 | 0/0 | 2.5 | 869.5 |
| 21/M | 54/12 | 55/25 | 3/0 | 3/0 | 2.5 | 950 |
| 22/F | 67/7 | 45/28 | 2/1 | 4/2 | 3 | 650 |
| 23/M | 67/12 | 63/42 | 2/1 | 2/0 | 3 | 675 |
| 24/M | 58/9 | 32/10 | 2/0 | 0/0 | 2.5 | 781.75 |
| 25/F | 59/30 | 73/41 | 4/2 | 4/4 | 3 | 537.5 |
| 26/F | 65/20 | 72/45 | 3/3 | 3/0 | 3 | 1200 |
| 27/M | 61/8 | 79/40 | 2/0 | 4/0 | 3 | 550 |
| 28/F | 71/5 | 67/40 | 2/1 | 0/0 | 2.5 | 187.5 |
| 29/M | 52/3 | 26/9 | 1/0 | 0/0 | 2 | 300 |
| 30/F | 76/3 | 47/22 | 2/1 | 0/0 | 2 | 300 |

[a]Gait and FOG at 12 hours' withdrawal of parkinsonism medication (*off*) and 1–2 h after the administration of L-dopa (*on*) states.
Abbreviations: UPDRS-III, Movement Disorder Society–revised Unified Parkinson's Disease Rating Scale Part III; FOG, freezing of gait; HY, Hoehn and Yahr; LED, L-dopa equivalent dose; M, male; F, female.

duration were examined and reported in Supporting Information Data S1.

## Task Paradigm

The task paradigm comprised three locomotion states (sitting, standing, and walking) within a single recording session where EEG and EMG were acquired under both *off* and *on* L-dopa states. The *off* L-dopa state was defined as at least 12 hours of medication withdrawal, whereas the *on* L-dopa state was assessed 1 to 2 hours after L-dopa intake of a challenge dose (150%; see Table 1 for details). Participants sat quietly for more than 1 minute and then stood for more than

1 minute. For the walking condition, they walked back and forth over a distance of 5 m for 5 minutes. All participants completed the sitting and walking tasks in the *on* L-dopa state, whereas only 24 completed the standing task. In the *off* L-dopa state, 26 participants completed the sitting and walking tasks, and 21 completed the standing task.

## Data Recording

EEG was recorded using a 10–20 system cap with an embedded reference electrode (FCz) and additional electrodes at C1 and C2, totaling 23 channels. For analysis, channels C1, C2, and Cz, located near the primary motor cortex (M1), were selected because of their established relevance to lower-limb motor functions.[37-40] The remaining channels were used to ensure signal quality, support noise removal, and allow for channel interpolation when needed. EMG signals were recorded from the gastrocnemius muscle, which is crucial for maintaining balance during the heel strike[41] and plays a vital role during the push-off phase. These neuroelectrophysiological measurements are referred to as cEEG (C1, C2, Cz) and gEMG throughout this article. Both EEG and EMG were sampled at 512 Hz using the Compumedics Neuroscan Grael EEG 2 system. Foot pressure data were acquired and processed using a custom system described in Supporting Information Data S1.

## Data Processing

Initial analyses were conducted on 1-minute continuous data for each locomotion state (sitting, standing, and walking). Walking data were then further segmented into individual steps using footpad pressure sensor triggers, and 20 clean straight-walking steps with both feet were chosen for individual step analysis. The gait cycle interval was defined as the time between consecutive heel strikes from the same foot. Because step length could not be measured directly by the sensors, video recordings were used to count the number of steps between two fixed 5-m landmarks, with the mean step length calculated by dividing the distance by the number of steps. All EEG data were filtered, average referenced, and cleaned using independent component analysis to remove nonbrain artifact components and retain "brain" components as labeled by ICLabel.[42] The focus on selected central lobe channels could also help to reduce neck-related movement artifacts. Additional artifact rejection criteria, including peak-to-peak thresholds and mean/standard deviation (SD) outlier removal, were applied to exclude noisy epochs. Subsequently, time-frequency representations were visually inspected to ensure that no cross-frequency artifacts were included in the analysis. All further analyses were performed on channel level and then averaged. All event-related analyses were time locked to heel strikes, using EMG from the ipsilateral muscles and EEG from the contralateral hemisphere. The processing was done by using MNE-Python.[43] Detailed descriptions of the preprocessing methods are provided in Supporting Information Data S1.

## Phase-Amplitude Coupling

To investigate PAC, we employed the Gaussian Copula PAC (GC-PAC) method from Tensorpac,[44] which is well suited for analyzing short-duration data between different signal sources:

$$gcPAC = I(a(t); [\sin(\phi(t)), \cos(\phi(t))]) \quad (1)$$

The method first applies a copula normalization to transform the phase and amplitude data into a standard normal distribution. This step mitigates variations in amplitude scaling and signal-to-noise ratios across modalities, allowing for a robust, bias-corrected Gaussian estimation of mutual information. The step-related PAC was calculated using the event-related PAC measure, which employs a circular-linear correlation approach. This method evaluates the Pearson correlation across trials between the amplitude and the sine and cosine of the phase:

$$\begin{aligned} r_{sx} &= c(\sin(\phi_t), a_t), r_{cx} = c(\cos(\phi_t), a_t), \text{and } r_{sc} \\ &= c(\sin(\phi_t), \cos(\phi_t)) \end{aligned} \quad (2)$$

$$\rho_{cl} = \sqrt{\frac{r_{sx}^2 + r_{cx}^2 - 2 r_{sx} r_{cx} r_{sc}}{1 - r_{sc}^2}} \quad (3)$$

## Statistical Analysis

We employed two complementary approaches: an evidence-based method that replicated baseline results using established bandwidths (eg, alpha: 8–12 Hz, beta: 12–30 Hz, and gamma: 40–200 Hz) from previous studies,[29,45] and a data-driven method using permutation and surrogate testing to identify frequency bands sensitive to specific L-dopa and locomotion conditions.

A two-way analysis of variance (ANOVA) was conducted to assess the main and interaction effects between L-dopa state (*off* vs. *on*) and locomotion state (sitting, standing, walking) on the powers and PAC. For post hoc comparisons, the nonparametric test Mann–Whitney *U* was employed. A cluster-based permutation test with 2000 iterations was employed to identify statistically significant differences in powers/PAC. EEG and EMG time-frequency decompositions were permuted between walking steps and random, same-length segments from sitting. The original data were permuted at the step segment level between *off* and *on* conditions, and then PAC was recalculated to generate a null distribution. Significant step-related

PAC clusters in each L-dopa state were identified by comparing the target PAC with its phase-signal surrogates. We first used a generalized linear model (GLM) to examine the association between measured gait symptoms and UPDRS-III attributes. Subsequently, the GLM was employed to identify which PAC measure—derived from different locomotion conditions—best predicts motor symptoms, including UPDRS-III scores, step length, and gait cycle intervals. Pearson correlation assessed linear relationships between variables. $z$ score outlier removal with a threshold of 3 was used to ensure data quality by eliminating data points. The false discovery rate (FDR) was controlled for multiple comparisons using the Benjamini-Hochberg with error rate set to 0.05 ($\alpha = 0.05$). The original results were reported in the figures, and results with FDR-corrected $P$ values specified in annotations.

# Results

## Behavior Measurements

The Mann–Whitney $U$ test showed a significantly longer gait cycle interval ($U = 491.0$, $P = 0.0285$; Fig. 1A) and shorter step length ($U = 182.0$, $P = 0.0028$) in the *off* compared with *on* L-dopa state (Fig. 1C). Pearson correlation analyses demonstrated that both gait cycle intervals ($r = 0.4243$, $P = 0.0308$; Fig. 1B) and step length ($r = -0.5797$, $P = 0.0024$; Fig. 1D) correlated with UPDRS-III scores in the *off* state, indicating significant influence of PD symptoms on these walking patterns. GLM regression further indicated that the gait cycle interval increase might be ascribed to rigidity ($\beta = 0.0140$, $P = 0.0405$, FDR-adjusted $P = 0.1620$; akinesia: $\beta = -0.0042$, $P = 0.3597$; tremor: $\beta = 0.0046$, $P = 0.1432$; gait: $\beta = 0.0083$, $P = 0.3651$), although this did not survive multiple comparisons correction, whereas shorter step length remained significantly linked to higher UPDRS-III subsection gait scores (gait: $\beta = 1.6998$, $P = 0.0018$, FDR-adjusted $P = 0.0073$; rigidity: $\beta = -0.0006$, $P = 0.9082$; akinesia: $\beta = -0.0041$, $P = 0.2214$; tremor: $\beta = 0.0009$, $P = 0.7009$). L-Dopa treatment significantly improved motor performance, with an average 41.34% reduction in the UPDRS-III score. The improvement was observed across various motor symptoms, with reductions of 38.24%, 41.50%, 44.50%, and 53.27% in rigidity, akinesia, tremor, and gait, respectively ($P < 0.01$).

## Central EEG and Gastrocnemius EMG Powers

A two-way ANOVA indicated significant main effects of L-dopa ($F = 7.5470$, $P = 0.0070$) and locomotion ($F = 220.8337$, $P < 0.0001$) on gEMG gamma band (40–200 Hz), as well as a significant interaction effect between L-dopa and locomotion ($F = 5.0968$, $P = 0.0075$). Post hoc tests confirmed a substantial decrease in gEMG power during the *on* compared with *off* L-dopa state while sitting ($U = 393.0$, $P = 0.0047$, FDR-adjusted $P = 0.0061$), whereas no significant differences were observed during standing ($U = 140.0$, $P = 0.4408$) or walking ($U = 248.0$, $P = 0.7332$). Movement significantly increased gEMG power from sitting to standing and then walking in both *off* and *on* L-dopa states ($P < 0.0001$, FDR-adjusted $P < 0.0001$).

Conversely, a two-way ANOVA showed a significant effect of locomotion on cEEG alpha ($F = 3.1583$, $P = 0.0459$) and broad gamma band power ($F = 7.2906$, $P = 0.0010$). No significant L-dopa effects were observed in any specific band. Post hoc comparisons showed that alpha power was reduced during walking compared with sitting, especially when *on* medication ($U = 439.0$, $P = 0.0127$, FDR-adjusted $P = 0.1145$; Fig. 2A). In contrast, gamma band power increased during walking compared with sitting in both *on* ($U = 186.0$, $P = 0.0034$, FDR-adjusted $P = 0.0308$; Fig. 2A) and *off* L-dopa states ($U = 160.0$, $P = 0.0228$, FDR-adjusted $P = 0.1028$; Fig. 2A). The power spectrum density (PSD) analysis of the cEEG demonstrated a decrease within the alpha and beta bands as participants transitioned from sitting to standing to walking, but permutation testing showed no frequency-specific differences reaching statistical significance (Fig. 2B). In addition, we investigated how cEEG and gEMG activities were modulated within the gait cycle. Significant modulations were observed in alpha and beta band power in the cEEG within a single gait cycle during both *on* and *off* L-dopa states, with both alpha and beta activity decreasing before the contralateral heel strike and increasing afterward (Fig. 2C).

## Central EEG Alpha/Beta-Gamma PAC

We observed an increase in cEEG beta-broad gamma PAC in the *off* L-dopa state compared with the *on* L-dopa state, particularly during standing (Fig. 3A). Specifically, phase modulation was most prominent around 10 Hz. However, to maintain consistency with previous studies, we initially adopted a hypothesis-driven approach, focusing on the beta frequency range (12–30 Hz) for phase and broad gamma range (40–200 Hz) for amplitude. A two-way ANOVA on data within these frequency bands confirmed a significant main effect of L-dopa ($F = 4.7642$, $P = 0.0306$) and an interaction effect between L-dopa and locomotion ($F = 4.2484$, $P = 0.0161$), whereas the main effect of locomotion was not significant ($F = 2.6811$, $P = 0.0718$). Specifically, L-dopa significantly reduced beta-gamma PAC, with the effect most pronounced during standing, although this reduction did not survive FDR correction ($U = 339.0$, $P = 0.0227$, FDR-adjusted $P = 0.0680$; Fig. 3B). In the *off* L-dopa state, beta-gamma PAC during standing increased significantly compared with sitting ($U = 148.0$,

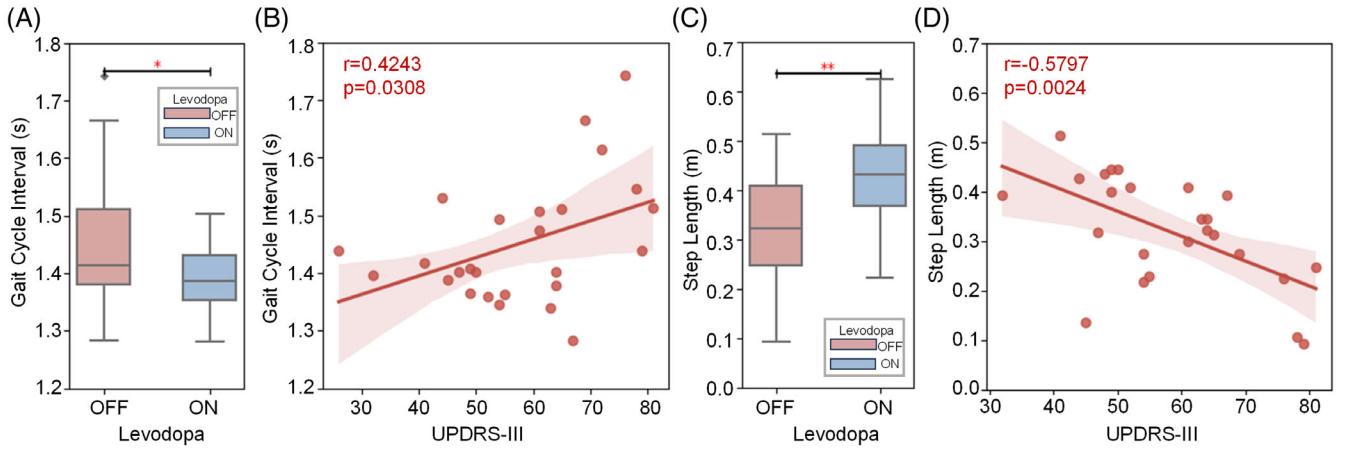


**FIG. 1.** Statistics of gait cycle intervals and step length. Significance levels were determined based on the original *P* values (without false discovery rate [FDR] correction). Values that passed the FDR threshold are indicated in red, whereas those that did not pass are presented in black. (**A**) The gait cycle intervals in the *on* L-dopa state are significantly shorter than those in the *off* L-dopa state. (**B**) The gait cycle intervals in the *off* L-dopa state show a significant correlation with Movement Disorder Society–revised Unified Parkinson's Disease Rating Scale Part III (UPDRS-III) scores. (**C**) The step lengths in the *off* L-dopa state are significantly shorter than those in the *on* L-dopa state. (**D**) The step lengths in the *off* L-dopa state are significantly correlated with UPDRS-III scores. [Color figure can be viewed at wileyonlinelibrary.com]

$P = 0.0119$, FDR-adjusted $P = 0.0537$), although not after FDR correction. In the *on* L-dopa state, beta-gamma PAC during walking decreased significantly compared with sitting ($U = 625.0$, $P = 0.0041$, FDR-adjusted $P = 0.0366$). In the off l-dopa state, higher central EEG β–γ PAC was associated with higher UPDRS-III scores during sitting (β = 43.9625, P = 0.0302, FDR-adjusted P = 0.0453) and standing (β = 19.0411, P = 0.0203, FDR-adjusted P = 0.0453), but not walking (β = −1.1020, P = 0.8914), in the off L-dopa state (Fig. 3C).

To explore the frequency range with the most significant phase modulation, we averaged PAC across the broad gamma range (40–200 Hz). This analysis identified a significant difference in the phase modulation frequency band from 8.5 to 17.0 Hz ($P < 0.05$; Fig. 3D), corresponding to the alpha/low-beta frequency band. This PAC was subsequently averaged across phase frequencies for post hoc tests that indicated a significant increase in PAC in the *off* compared with *on* L-dopa state during walking ($U = 435.0$, $P = 0.0332$). The Pearson correlation analysis showed a significant correlation between alpha/low beta (8.5–17.0 Hz) to broad gamma (40–200 Hz) PAC and UPDRS-III scores ($r = 0.4284$, $P = 0.0467$; Fig. 3E).

Permutation testing of the frequency-resolved PAC spectrum showed a narrowband peak coupling at 7.5 to 11.5 Hz phase and 93 to 117 Hz amplitude. This narrowband gamma PAC increased *off* versus *on* L-dopa difference significance ($P = 0.0015$; Fig. 3F) and positively correlated with UPDRS-III with a lower *P* value ($r = 0.5162$, $P = 0.0139$; Fig. 3G). When the 93 to 117 Hz window was notched out, the correlation between low-frequency phase and "broad" (40–200 Hz) gamma PAC vanished ($P = 0.2735$). In a GLM containing both predictors, only narrowband gamma remained explanatory (β = 20.3476, $P = 0.14$), whereas the broadband term was negligible (β = −0.82, $P = 0.96$), confirming that the apparent broadband effect is driven by the narrowband gamma.

## cEEG Beta-gEMG Gamma PAC

Both L-dopa and locomotion had main effects on cEEG-gEMG beta-gamma PAC ($F = 4.9622$, $P = 0.0274$; $F = 45.2271$, $P < 0.0001$). However, no interaction effect between L-dopa and locomotion was observed ($P = 0.8929$; Fig. 4A). Post hoc test demonstrated the significant reduction impact of L-dopa on cEEG-gEMG PAC only during walking ($U = 532.0$, $P = 0.0092$, FDR-adjusted $P = 0.0138$), but showed no significant effect during sitting or standing ($P = 0.1553$, $P = 0.3451$). The cEEG-gEMG beta-gamma PAC decreased significantly during walking compared with both sitting ($U = 535.0$, $P = 0.0003$, FDR-adjusted $P = 0.0007$, *off*; $U = 737.0$, $P < 0.0001$, FDR-adjusted $P < 0.0001$, *on*) and standing ($U = 530.0$, $P < 0.0001$, FDR-adjusted $P < 0.0001$, *off*; $U = 665.0$, $P < 0.0001$, FDR-adjusted $P < 0.0001$, *on*), independently of L-dopa state. In the *off* L-dopa state, GLM demonstrated that increased cEEG-gEMG beta-gamma PAC during walking was significantly associated with higher UPDRS-III scores ($\beta = 76.0980$, $P = 0.0035$, FDR-adjusted $P = 0.0106$; Fig. 4B), whereas no such association was observed during sitting ($\beta = -3.7152$, $P = 0.7560$) or standing ($\beta = 5.9677$, $P = 0.5615$). Moreover, the average cEEG-gEMG PAC during walking negatively correlated with step length in the *off* L-dopa state, where increased cEEG-gEMG beta-gamma PAC was associated with shorter step lengths during

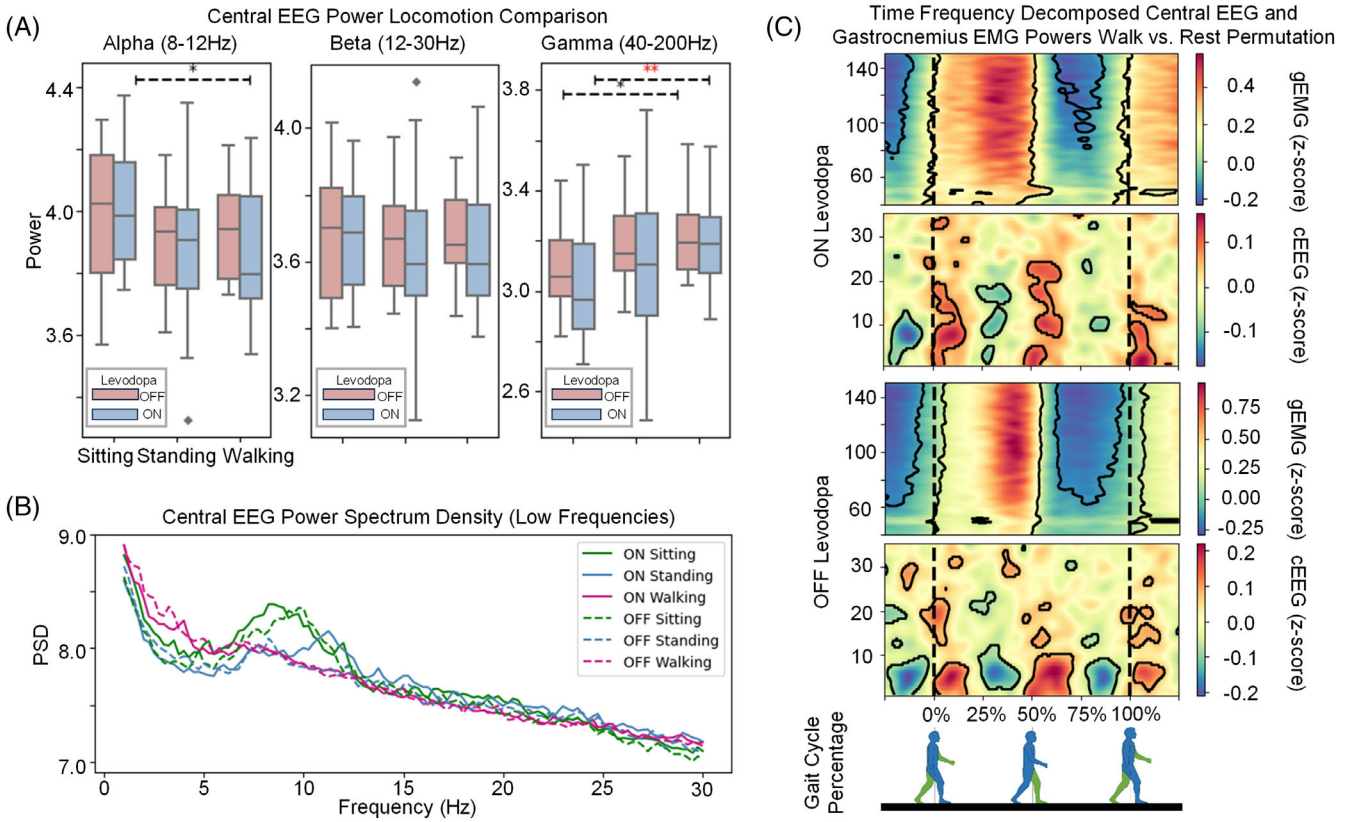


**FIG. 2.** EMG and EEG power analysis. Values that passed the false discovery rate (FDR) threshold are indicated in red, whereas those that did not pass are presented in black. (**A**) For the averaged EEG power analysis across C1, C2, and Cz channels, only locomotion and not medication leads to significant changes in power. Alpha band power significantly decreases during walking compared with sitting at rest in the *on* L-dopa state. Conversely, gamma band power significantly increases during walking in both the *off* and *on* L-dopa states. All values are processed with log10 + 5 for improved presentation. (**B**) Power spectrum density (PSD) of central lobes EEG: The PSD in alpha and beta bands decreases from sitting to standing to walking, but no significant differences were observed among various locomotions or between *off* and *on* L-dopa status. (**C**) Gait cycle power spectra aligned to heel strikes as starter (time 0) showed a prominent event-related modulation especially in the alpha and beta frequency band during *on* L-dopa. EEG powers were averaged over the contralateral side of heel strike (C2, Cz for the left heel strike, C1, Cz for the right heel strike), then further averaged between two sides of the body. EMG was recorded from the ipsilateral gastrocnemius of heel strikes. The gait cycle percentage was demonstrated only on the lateral side for better presentation, with blue indicating the right foot and green the left foot. The start and end time points correspond to consecutive heel strikes, and the power spectrum was *z* score normalized before plotting. cEEG, central electroencephalogram; gEMG, gastrocnemius electromyography. [Color figure can be viewed at wileyonlinelibrary.com]

walking ($\beta = -0.5576$, $P = 0.0066$, FDR-adjusted $P = 0.0197$; Fig. 4C). However, GLM analysis did not demonstrate any significant associations between step length and cEEG-gEMG beta-gamma PAC during sitting ($\beta = 0.1149$, $P = 0.2185$) or standing ($\beta = 0.0582$, $P = 0.4653$; Fig. 4C).

When examining the decomposed PAC averaged across gEMG amplitude frequencies (40–200 Hz), significant modulation phases were confined to the 12.0 to 15.0 Hz range, corresponding to the cEEG low beta frequency (Fig. 4D). Further paired analysis confirmed significant differences between *off* and *on* L-dopa states ($U = 478.0$, $P = 0.0207$) during walking in the cEEG low beta (12.0–15.0 Hz) and gEMG broad gamma (140.0–200.0 Hz) PAC. Moreover, cEEG-gEMG PAC in the *off* condition significantly correlated with UPDRS-III scores ($r = 0.5025$, $P = 0.0145$; Fig. 4E). This frequency-specified cEEG-gEMG PAC also significantly correlates with step length ($r = -0.490$, $P = 0.0206$; Fig. 4F).

Permutation-based analysis of the cEEG-gEMG PAC spectrum showed a significant cluster centered on 13 to 14.5 Hz phase and 134 to 200 Hz amplitude, consistent with a broadband high-gamma component. Figure 4G presents the step-related PAC during the gait cycle. Surrogate testing showed significant time-locked contours in the *on* L-dopa state, indicating increased cEEG alpha/beta-gEMG gamma PAC during contralateral heel strike ($P < 0.05$). The permutation test confirmed the significance of these increases during *on* L-dopa compared with *off* condition.

## Discussion

This study introduces a novel, noninvasive system for monitoring cortical activities and corticomuscular interactions in patients with PD during sitting, standing, and free walking. Our results confirm the pathological

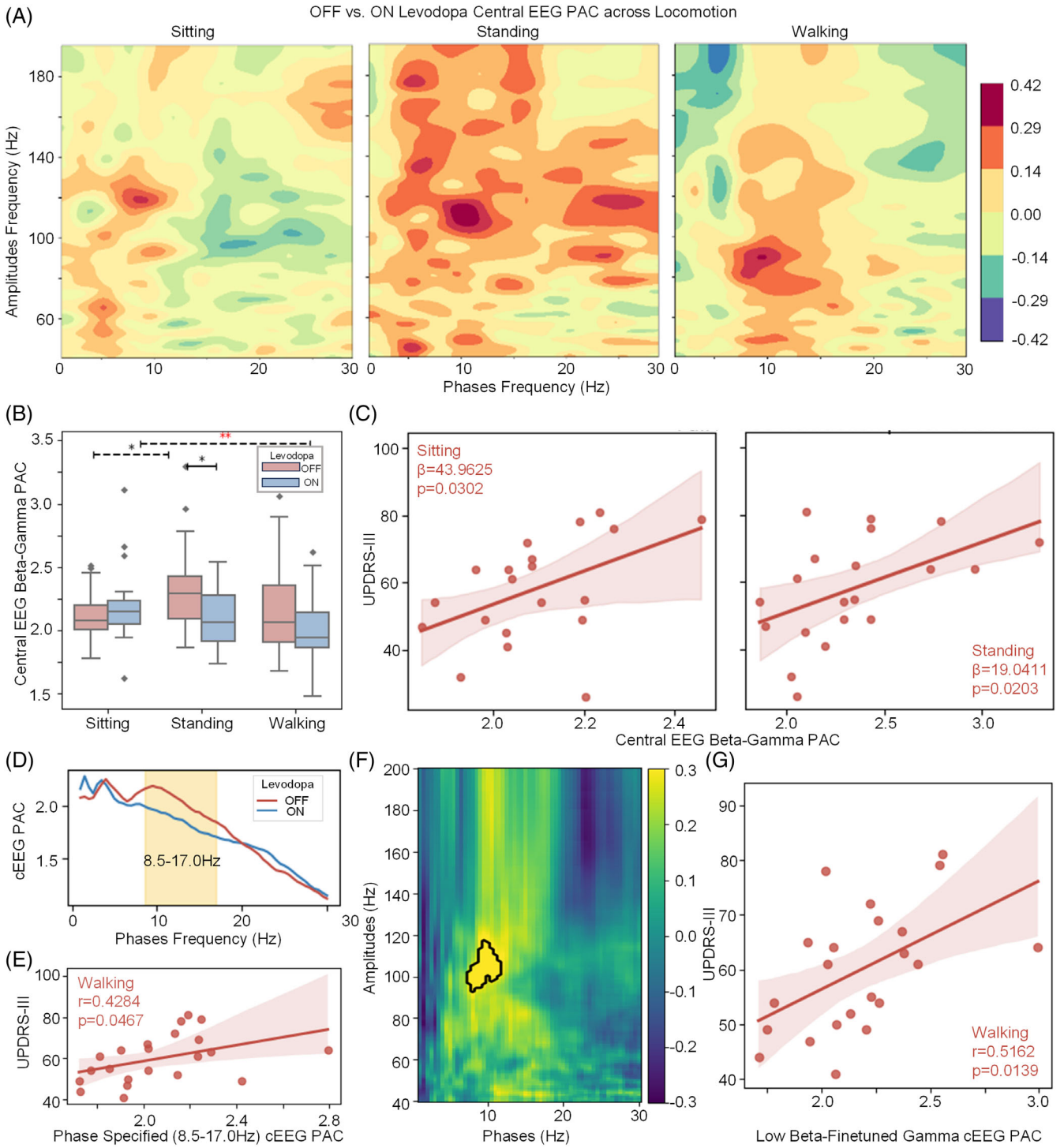


**FIG. 3.** Phase-amplitude coupling (PAC) results for central electroencephalogram (cEEG). The PAC values were processed with log10 + 5 for improved presentation. Significance levels were determined based on the original *P* values (without false discovery rate [FDR] correction). Values that passed the FDR threshold are indicated in red, whereas those that did not pass are presented in black. (**A**) The *off* versus *on* PAC during various locomotions illustrates a high contour around alpha/beta phase and gamma amplitude. (**B**) A two-way ANOVA demonstrates a significant effect of L-dopa and an interaction between L-dopa and movement state on cortical beta (12–30 Hz) to gamma (40–200 Hz) PAC. Post hoc test further showed significant differences between *off* and *on* states when standing. (**C**) A generalized linear model (GLM)-based multiple regression model demonstrates that *off* L-dopa sitting and standing PAC correlated with Movement Disorder Society–revised Unified Parkinson's Disease Rating Scale Part III (UPDRS-III) scores in the *off* L-dopa state. (**D**) The frequency decomposed walking cortical PACs were further averaged across 40–150 Hz in amplitudes dimension to explore the significantly different phase frequencies. The permutation test shows that during walking cortical PAC at phase frequencies of 8.5–17.0 Hz is significantly higher in the *off* L-dopa state compared with the *on* L-dopa state. (**E**) *Off* L-dopa averaged alpha/low beta to broadband gamma PACs during walking were significantly correlated with UPDRS-III overall scores ($P = 0.0467$). (**F**) Permutation test on frequency decomposed walking cortical PAC identifies significantly different areas between *off* and *on* L-dopa states, specifically around phase frequencies of 7.5–11.5 Hz and amplitude frequencies of 93.0–117.0 Hz. (**G**) Scatterplot showing the positive correlation between low beta-gamma PAC (*off* L-dopa) and UPDRS-III scores during walking ($r = 0.5162$, $P = 0.0139$). [Color figure can be viewed at wileyonlinelibrary.com]

significance of cortical beta-gamma PAC, as well as cortical beta-gEMG gamma PAC, in the motor symptoms and gait impairments in PD. Both of these cross-frequency couplings were found to be increased in the *off* L-dopa state, correlating with UPDRS scores and reduced step length during free walking. These findings are consistent with previous studies reporting increased cortical beta-gamma PAC in PD, measured via EEG, MEG,[25,26,46,47] or ECoG,[29,48] further supporting its potential as a biomarker for motor impairment and FOG. We also demonstrated dynamic fluctuation of cortical beta-EMG gamma PAC within each step cycle when patients were *on* L-dopa, with relatively increased corticomuscular beta-gamma PAC around heel strikes. In contrast, when *off* medication, this corticomuscular coupling remained high and stable throughout the step cycle without dynamic fluctuations. These results offer new insights into how cross-frequency and cross-region coupling are modulated not only by L-dopa but also different locomotion states and the specific dynamics within each step cycle during free walking.

## Locomotion Status–Dependent Modulation of Cortical Alpha/Low Beta-Gamma PAC Is Impacted by L-Dopa in PD

Elevated cortical alpha/low beta to gamma PAC during sitting has been previously associated with higher UPDRS-III scores.[49] In addition, Yin et al[29] observed enhanced low beta-gamma PAC in the motor cortex during standing and at the onset of FOG. This enhancement was attributed to beta hypersynchrony in the basal ganglia, which likely drives stronger beta-gamma coupling in the motor cortex.[50] Our results also suggest that cEEG beta-gamma PAC is a more reliable predictor for UPDRS scores when quantified during sitting and standing than during walking. This is consistent with previous studies[29,30,51,52] and suggests that cEEG PAC may serve as a more stable indicator of symptom severity in static postures. Although cortical beta-gamma PAC significant differences between *off* and *on* conditions during standing were observed, they did not survive FDR correction, warranting further investigation into their potential as biomarkers. In addition, our data-driven approach highlighted a broader modulatory frequency band, including both alpha and low-beta (8.5–17.0 Hz), modulating broad gamma activity (40–200 Hz) in the cortex. This PAC was significantly higher in the *off* L-dopa state compared with *on* L-dopa during walking and correlated with motor symptom severity, as reflected by higher UPDRS-III scores. These findings suggest that the frequency bandwidth of PAC changes associated with symptom severity and L-dopa effects may vary depending on the locomotion context. By statically isolating 7.5 to 11.5 Hz and 93 to 117 Hz coupling, we show that L-dopa specifically restores a narrowband cortical gamma PAC that tracks UPDRS-III during free walking. In PD, broadband gamma (≈50–200 Hz) appears as a smooth 1/*f*-like elevation reflecting asynchronous multiunit spiking and overall cortical excitability,[53] whereas finely tuned gamma is normally seen as true rhythmic oscillations generated by synchronized interneuron–pyramidal loops, is enhanced by dopaminergic therapy or DBS, and correlates closely with motor performance and symptom severity.[10,54] However, it should be noted that the statically identified narrowband gamma in PAC in this study may simply reflect the most consistent phase-locked frequency range to alpha/low beta across participants during free walking.

## Cortical Low Beta-Muscular Gamma PAC Reflects Motor Symptom Severity During Free Walking in PD and Is Selectively Enhanced by L-Dopa at the Heel-Strike Phase

Interestingly, corticomuscular beta-gamma PAC was reduced during walking compared with sitting and standing, with this reduction appearing independent of L-dopa state. In previous studies, cortical beta was found to be a "promoter of status quo,"[5,55] whereas gamma rhythms track active muscle contraction.[36] The observed reduction in corticomuscular beta-gamma PAC during walking may reflect a functional uncoupling of cortical beta from muscular gamma to permit dynamic motor adjustments. The loss of dopamine could contribute to the increase in aberrant corticomuscular beta-gamma coupling during walking. Further GLM analysis confirmed that this increase was associated with severe motor impairment (higher UPDRS-III scores) and worsened gait (shorter step length). These findings suggest that corticomuscular beta-gamma PAC during walking could serve as a key marker of both L-dopa status and symptoms severity. Furthermore, our data-driven approach indicated that cortical low beta (12–15 Hz) and muscular gamma PAC was specifically elevated during walking in the *off* L-dopa state, and this was positively correlated with motor symptom severity, highlighting its role in the pathophysiology of free walking. The corticomuscular PAC in the amplitude frequency band lacks a narrow spectral peak and instead shows a smooth, broadband increase, reflecting observed corticomuscular PAC in this range primarily indexes peripheral muscle activation strength.

In addition, we observed dynamic fluctuation in corticomuscular alpha/low beta-gamma PAC within the gait cycle, but only in the *on* and not *off* L-dopa state. This suggests that selective enhancement of corticomuscular PAC during heel striking within the gait cycle may play a key functional role under dopaminergic influence. This is consistent with previous findings showing that

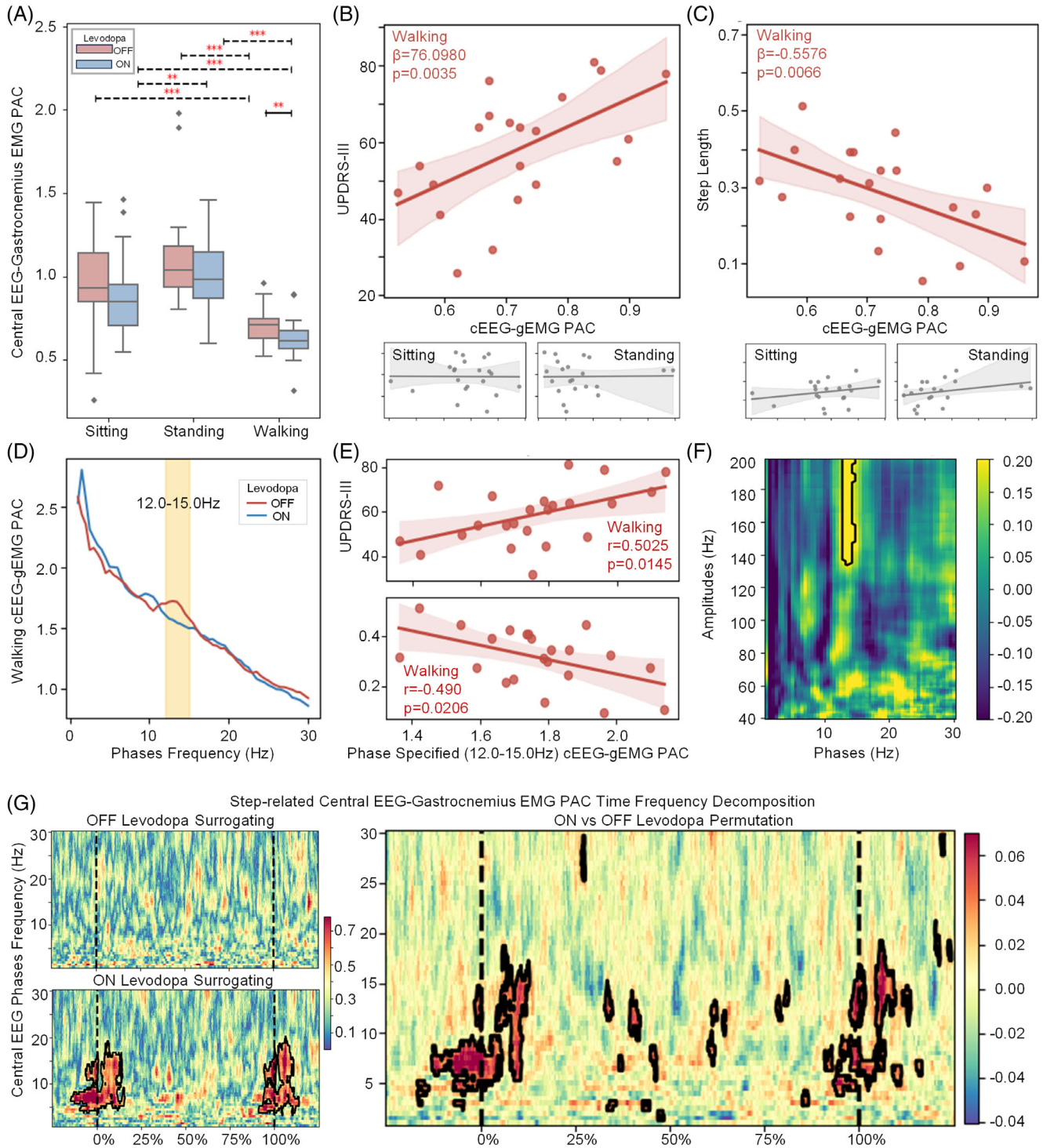


**FIG. 4.** Phase-amplitude coupling (PAC) results for cEEG-gEMG. The PAC values are processed with log10 + 5 for better presentation. Significance levels were determined based on the original *P* values (without false discovery rate [FDR] correction). Values that passed the FDR threshold are indicated in red, whereas those that did not pass are presented in black. (**A**) A comparison of averaged beta (12–30 Hz) to broadband gamma (40–200 Hz) PACs across L-dopa and gesture conditions shows a significant reduction in corticomuscular PACs during walking in the *on* L-dopa state compared with the *off* L-dopa state, with walking exhibiting lower PACs than sitting in both states. (**B**) Generalized linear model (GLM) analysis demonstrates a significant correlation between *off* L-dopa walking PACs and Movement Disorder Society–revised Unified Parkinson's Disease Rating Scale Part III (UPDRS-III) scores, but not sitting and standing. (**C**) GLM analysis also shows the walking step length is specifically correlated with walking cEEG-gEMG PAC during *off* conditions. (**D**) Analysis of phase frequencies highlights a 12–15 Hz low beta band difference between L-dopa states in walking corticomuscular PAC. (**E**) The data-driven determined phase frequency band walking cEEG-gEMG PAC shows significant correlations to UPDRS-III in the *off* L-dopa state ($P = 0.0145$). Frequency-specified walking cEEG-gEMG PACs in the *off* L-dopa state significantly correlate with the walking step length ($P = 0.0206$). (**F**) Permutation testing identifies significant walking corticomuscular PAC differences between 13.0–14.5 Hz (phase) and 135.0–200.0 Hz (amplitude) frequencies, with higher values observed in the *off* L-dopa state. Significant areas are highlighted by black contours. (**G**) Step-based PAC analysis shows significant cEEG-gEMG alpha/beta-gamma coupling around heel strikes. The permutation test confirmed these increased modulations are more significant in *on* than *off* L-dopa. cEEG, central electroencephalogram; gEMG, gastrocnemius electromyography. [Color figure can be viewed at wileyonlinelibrary.com]

activities in the STN,[56] pedunculopontine nucleus (PPN),[45] and motor cortex are dynamically modulated within the step cycle. L-Dopa appears to suppress baseline corticomuscular beta-gamma PAC and restores dynamic cortical beta gating. As a result, phasic alpha/low beta-gamma PAC peaks reappear at key stages, such as the heel strike, facilitating more precise muscle control. These PAC enhancements, occurring in different temporal contexts, may have distinct functional implications. Our results align with previous work suggesting that temporally targeted interventions, such as alternating DBS[57,58] or gait phase-locked DBS, may offer improved therapeutic outcomes for gait impairments in PD.

## Limitations

This study has several limitations. First, recordings were relatively short and confined to a laboratory setting. It remains to be tested whether the reported results generalize to everyday life, where motor behavior is more diverse. Second, we used central lobe EEG to noninvasively monitor cortical activity over the motor regions. However, the scalp and skull introduce resistance that can influence recorded signals. Therefore, the measured activity likely reflects cortical electrical field potentials rather than direct neural sources. This limits the precision with which we can interpret EEG data as a direct readout of cortical processes. Future work could improve spatial resolution by incorporating high-density EEG or invasive methods such as stereo-EEG or ECoG. Third, the reported correlations between beta-gamma PAC and motor impairment were based on cross-participant correlations. Although informative at the group level, these do not capture individual variability over time. This is particularly important for establishing PAC as a real-time biomarker for applications such as adaptive DBS (aDBS), which requires sensitivity to within-subject fluctuations in symptom severity. Despite these limitations, our current results offer promising support for PAC as an objective biomarker of motor impairment in PD. Nevertheless, further work is needed to determine its reliability and specificity at the individual level. Future research should aim to include longer, real-world recordings and adopt within-subject analyses to more fully explore the potential of PAC as a dynamic and personalized biomarker for PD and its application in aDBS.

## Conclusions

This study identifies enhanced alpha/low beta-gamma PAC in both cortical and corticomuscular networks as potential biomarkers for PD. Altered walking-related PAC interactions, particularly during L-dopa withdrawal, suggest that increased beta-gamma coupling may contribute to motor and gait impairments in PD. The sensitivity of alpha/beta-gamma PAC to medication status highlights its potential utility for assessing therapeutic efficacy and informing targeted interventions. Furthermore, the application of noninvasive, dynamic monitoring, particularly during gait, presents a promising avenue for the development of clinically relevant biomarkers. Such approaches may ultimately enable more precise, closed-loop systems for tracking and modulating neural and muscular activity in real time, with the goal of improving clinical outcomes in patients with PD.

**Author Roles:** H.Z.: Writing—original draft, visualization, methodology, investigation, formal analysis, data curation, conceptualization, and funding acquisition. S. Hao: Writing—review and editing, methodology, visualization, investigation, and data curation. P.Z.: Writing—review and editing, visualization, methodology, and data curation. S. He: Writing—review and editing and methodology. L.W.: Writing—review and editing and statistics. Z.F.: Writing—review and editing, investigation, data curation, and resources. L.X.: Investigation, data curation, and resources. S.Z.: Data curation and resources. W.L.: Data curation and resources. X.Z.: Data curation and resources. M.-L.W.: Writing—review and editing. D.L.: Data curation and resources. B.S.: Data curation and resources. Y.L.: Resources, funding acquisition, and supervision. H.T.: Writing—review and editing, methodology, conceptualization, and supervision. C.C.: Writing—review and editing, methodology, conceptualization, supervision, resources, and funding acquisition.

**Acknowledgments:** This work was supported by the Postdoctoral Fellowship Program of CPSF under Grant GZC20231665 (to H.Z.), Shanghai Municipal Science and Technology Commission (21Y11905300 to B.S.), and the National Science Foundation of China (82071547 to C.C.). We acknowledge our patients for participating in this project, and Prof. Vladimir Litvak for constructive suggestions on analysis.

**Financial Disclosures:** S.H., L.W., and H.T were supported by the Medical Research Council (MRC) (MC_UU_00003/2), the Medical and Life Sciences Translational Fund (MLSTF) from the University of Oxford, the National Institute for Health and Care Research (NIHR) Oxford Biomedical Research Centre, and the Rosetrees Trust, UK. S.H. was also supported by a Non-Clinical Postdoctoral Fellowship from the Guarantors of Brain and an International Exchanges Award (IES\R3\213,123).

## Data Availability Statement

All relevant codes reported in the article can be freely accessed without restriction (https://github.com/hyphenzhao/PD_PAC_Biomarkers). The raw data that support the findings of this study are available from the corresponding author upon reasonable request after approval of the local ethics committee.

# References

1. The unified Parkinson's disease rating scale (UPDRS): status and recommendations. Mov Disord 2003;18:738–750.
2. Noh H, Kwon S, Cho SY, et al. Effectiveness and safety of acupuncture in the treatment of Parkinson's disease: a systematic review and meta-analysis of randomized controlled trials. Complement Ther Med 2017;34:86–103.
3. Bhidayasiri R, Martinez-Martin P. Clinical assessments in Parkinson's disease. Parkinson's Disease 2017;132:129–182. https://doi.org/10.1016/bs.irn.2017.01.001
4. Shirahige L, Berenguer-Rocha M, Mendonça S, Rocha S, Rodrigues MC, Monte-Silva K. Quantitative electroencephalography characteristics for Parkinson's disease: a systematic review. J Parkinsons Dis 2020;10:455–470.

5. Little S, Brown P. The functional role of beta oscillations in Parkinson's disease. Parkinsonism & Related Disorders 2014;20: S44–S48.
6. Trottenberg T, Fogelson N, Kühn AA, Kivi A, Kupsch A, Schneider GH, Brown P. Subthalamic gamma activity in patients with Parkinson's disease. Exp Neurol 2006;200:56–65.
7. Chen CC, Hsu YT, Chan HL, et al. Complexity of subthalamic 13–35Hz oscillatory activity directly correlates with clinical impairment in patients with Parkinson's disease. Exp Neurol 2010;224: 234–240.
8. Hammond C, Bergman H, Brown P. Pathological synchronization in Parkinson's disease: networks, models and treatments. Trends Neurosci 2007;30:357–364.
9. Brown P, Oliviero A, Mazzone P, Insola A, Tonali P, di Lazzaro V. Dopamine dependency of oscillations between subthalamic nucleus and pallidum in Parkinson's disease. J Neurosci 2001;21:1033–1038.
10. Swann NC, de Hemptinne C, Miocinovic S, et al. Gamma oscillations in the hyperkinetic state detected with chronic human brain recordings in Parkinson's disease. J Neurosci 2016;36:6445–6458.
11. Bouthour W, Mégevand P, Donoghue J, Lüscher C, Birbaumer N, Krack P. Biomarkers for closed-loop deep brain stimulation in Parkinson disease and beyond. Nat Rev Neurol 2019;15:343–352.
12. de Hemptinne C, Swann NC, Ostrem JL, Ryapolova-Webb ES, San Luciano M, Galifianakis NB, Starr PA. Therapeutic deep brain stimulation reduces cortical phase-amplitude coupling in Parkinson's disease. Nat Neurosci 2015;18:779–786.
13. Oswal A, Beudel M, Zrinzo L, et al. Deep brain stimulation modulates synchrony within spatially and spectrally distinct resting state networks in Parkinson's disease. Brain 2016;139:1482–1496.
14. Kilavik BE, Zaepffel M, Brovelli A, MacKay WA, Riehle A. The ups and downs of beta oscillations in sensorimotor cortex. Exp Neurol 2013;245:15–26.
15. Fernández A, Zuluaga P, Abásolo D, Gómez C, Serra A, Méndez MA, Hornero R. Brain oscillatory complexity across the life span. Clin Neurophysiol 2012;123:2154–2162.
16. Ishii R, Canuet L, Aoki Y, et al. Healthy and pathological brain aging: from the perspective of oscillations, functional connectivity, and signal complexity. Neuropsychobiology 2017;75:151–161.
17. Kilavik BE, Ponce-Alvarez A, Trachel R, Confais J, Takerkart S, Riehle A. Context-related frequency modulations of macaque motor cortical LFP Beta oscillations. Cereb Cortex 2011;22:2148–2159.
18. Boon LI, Geraedts VJ, Hillebrand A, Tannemaat MR, Contarino MF, Stam CJ, Berendse HW. A systematic review of MEG-based studies in Parkinson's disease: the motor system and beyond. Hum Brain Mapp 2019;40:2827–2848.
19. Shreve LA, Velisar A, Malekmohammadi M, et al. Subthalamic oscillations and phase amplitude coupling are greater in the more affected hemisphere in Parkinson's disease. Clin Neurophysiol 2017; 128:128–137.
20. van Wijk BCM, Beudel M, Jha A, et al. Subthalamic nucleus phase–amplitude coupling correlates with motor impairment in Parkinson's disease. Clin Neurophysiol 2016;127:2010–2019.
21. Sharott A, Grosse P, Kuhn AA, et al. Is the synchronization between pallidal and muscle activity in primary dystonia due to peripheral afferance or a motor drive? Brain 2008;131:473–484.
22. Tsiokos C, Malekmohammadi M, AuYong N, Pouratian N. Pallidal low β-low γ phase-amplitude coupling inversely correlates with Parkinson disease symptoms. Clin Neurophysiol 2017;128:2165–2178.
23. Meidahl AC, Moll CKE, van Wijk BCM, et al. Synchronised spiking activity underlies phase amplitude coupling in the subthalamic nucleus of Parkinson's disease patients. Neurobiol Dis 2019;127: 101–113.
24. Swann NC, de Hemptinne C, Aron AR, Ostrem JL, Knight RT, Starr PA. Elevated synchrony in <scp>P</scp>arkinson disease detected with electroencephalography. Ann Neurol 2015;78: 742–750.
25. Hodnik T, Roytman S, Bohnen NI, Marusic U. Beta–gamma phase-amplitude coupling as a non-invasive biomarker for Parkinson's disease: insights from electroencephalography studies. Life (Basel) 2024;14:391.
26. Mertiens S, Sure M, Schnitzler A, Florin E. Alterations of PAC-based resting state networks in Parkinson's disease are partially alleviated by levodopa medication. Front Syst Neurosci 2023;17:1219334.
27. Miller AM, Miocinovic S, Swann NC, et al. Effect of levodopa on electroencephalographic biomarkers of the parkinsonian state. J Neurophysiol 2019;122:290–299.
28. Rajagopalan SS, Miller AM, de Hemptinne C, San Luciano M, Ostrem JL, Starr PA. Washout of chronic therapeutic deep brain stimulation increases cortical phase-amplitude coupling. Parkinsonism Relat Disord 2019;66:269–271.
29. Yin Z, Zhu G, Liu Y, et al. Cortical phase-amplitude coupling is key to the occurrence and treatment of freezing of gait. Brain 2022;145: 2407–2421.
30. Kimoto Y, Tani N, Emura T, et al. Beta-gamma phase-amplitude coupling of scalp electroencephalography during walking preparation in Parkinson's disease differs depending on the freezing of gait. Front Hum Neurosci 2024;18:1495272.
31. dos Santos PCR, Heimler B, Koren O, Flash T, Plotnik M. Dopamine improves defective cortical and muscular connectivity during bilateral control of gait in Parkinson's disease. Commun Biol 2024; 7:495.
32. Airaksinen K, Mäkelä JP, Nurminen J, Luoma J, Taulu S, Ahonen A, Pekkonen E. Cortico-muscular coherence in advanced Parkinson's disease with deep brain stimulation. Clin Neurophysiol 2015;126:748–755.
33. Zokaei N, Quinn AJ, Hu MT, Husain M, van Ede F, Nobre AC. Reduced cortico-muscular beta coupling in Parkinson's disease predicts motor impairment. Brain Communications 2021;3:fcab179.
34. Hirschmann J, Özkurt TE, Butz M, Homburger M, Elben S, Hartmann CJ, et al. Differential modulation of STN–cortical and cortico-muscular coherence by movement and levodopa in Parkinson's disease. *NeuroImage* 2013;68:203–213.
35. Brown SP, Cron WL, Slocum JW. Effects of trait competitiveness and perceived Intraorganizational competition on salesperson goal setting and performance. J Mark 1998;62:88–98.
36. Patino L, Omlor W, Chakarov V, Hepp-Reymond M-C, Kristeva R. Absence of gamma-range Corticomuscular coherence during dynamic force in a deafferented patient. J Neurophysiol 2008;99: 1906–1916.
37. Ferreira C, Verst SM. Motor evoked potential. Intraoperative Monitoring: *Neurophysiology and Surgical Approaches*; Cham, Switzerland: Springer International Publishing; 2022:181–202. https://doi.org/10.1007/978-3-030-95730-8_9.
38. Presacco A, Forrester LW, Contreras-Vidal JL. Decoding intra-limb and inter-limb kinematics during treadmill walking from scalp electroencephalographic (EEG) signals. IEEE Trans Neural Syst Rehabil Eng 2012;20:212–219.
39. Gordleeva SY, Lobov SA, Grigorev NA, et al. Real-time EEG–EMG human–machine Interface-based control system for a lower-limb exoskeleton. IEEE Access 2020;8:84070–84081.
40. Ferrero L, Ortiz M, Quiles V, Iáñez E, Flores JA, Azorín JM. Brain symmetry analysis during the use of a BCI based on motor imagery for the control of a lower-limb exoskeleton. Symmetry 2021;13: 1746.
41. Elble RJ, Moody C, Leffler K, Sinha R. The initiation of normal walking. Mov Disord 1994;9:139–146.
42. Pion-Tonachini L, Kreutz-Delgado K, Makeig S. ICLabel: an automated electroencephalographic independent component classifier, dataset, and website. NeuroImage 2019;198:181–197.
43. Gramfort A, Luessi M, Larson E, Engemann DA, Strohmeier D, Brodbeck C, et al. MEG and EEG data analysis with MNE-Python. Frontiers in Neuroscience. 2013;267:1–13.
44. Combrisson E, Nest T, Brovelli A, Ince RAA, Soto JLP, Guillot A, Jerbi K. Tensorpac: an open-source python toolbox for tensor-based phase-amplitude coupling measurement in electrophysiological brain signals. PLoS Comput Biol 2020;16:e1008302.

45. He S, Deli A, Fischer P, et al. Gait-phase modulates alpha and Beta oscillations in the pedunculopontine nucleus. J Neurosci 2021;41: 8390–8402.

46. Muthukumaraswamy SD. Functional properties of human primary motor cortex gamma oscillations. J Neurophysiol 2010;104:2873–2885.

47. Gong R, Wegscheider M, Mühlberg C, et al. Spatiotemporal features of β-γ phase-amplitude coupling in Parkinson's disease derived from scalp EEG. Brain 2020;144:487–503.

48. de Hemptinne C, Ryapolova-Webb ES, Air EL, et al. Exaggerated phase–amplitude coupling in the primary motor cortex in Parkinson disease. Proc Natl Acad Sci USA 2013;110:4780–4785.

49. Tanaka M, Yanagisawa T, Fukuma R, et al. Magnetoencephalography detects phase-amplitude coupling in Parkinson's disease. Sci Rep 2022;12:1835.

50. O'Keeffe AB, Malekmohammadi M, Sparks H, Pouratian N. Synchrony drives motor cortex beta bursting, waveform dynamics, and phase-amplitude coupling in Parkinson's disease. J Neurosci 2020;40:5833–5846.

51. Tessitore A, Cirillo M, De Micco R. Functional connectivity signatures of Parkinson's disease. J Parkinsons Dis 2019;9:637–652.

52. Yu Y, Han F, Wang Q. Exploring phase–amplitude coupling from primary motor cortex-basal ganglia–thalamus network model. Neural Netw 2022;153:130–141.

53. Zhang J, Idaji MJ, Villringer A, Nikulin VV. Neuronal biomarkers of Parkinson's disease are present in healthy aging. NeuroImage 2021;243:118512.

54. Olaru M, Hahn A, Shcherbakova M, Little S, Neumann WJ, Abbasi-Asl R, Starr PA. Deep brain stimulation-entrained gamma oscillations in chronic home recordings in Parkinson's disease. Brain Stimul 2025;18:132–141.

55. Engel AK, Fries P. Beta-band oscillations—signalling the status quo? Curr Opin Neurobiol 2010;20:156–165.

56. Fischer P, Chen CC, Chang YJ, et al. Alternating modulation of subthalamic nucleus Beta oscillations during stepping. J Neurosci 2018; 38:5111–5121.

57. Fischer P, He S, de Roquemaurel A, et al. Entraining stepping movements of Parkinson's patients to alternating subthalamic nucleus deep brain stimulation. J Neurosci 2020;40:8964–8972.

58. Louie KH, Gilron R', Yaroshinsky MS, et al. Cortico-subthalamic field potentials support classification of the natural gait cycle in Parkinson's disease and reveal individualized spectral signatures. eneuro 2022;9:0325.

## Supporting Data

Additional Supporting Information may be found in the online version of this article at the publisher's web-site.